

PAPER • OPEN ACCESS

Magnetizing of Finemet-type alloys by magnetization rotation in weak fields

To cite this article: V A Kataev *et al* 2019 *J. Phys.: Conf. Ser.* **1389** 012120

View the [article online](#) for updates and enhancements.



IOP | ebooks™

Bringing together innovative digital publishing with leading authors from the global scientific community.

Start exploring the collection—download the first chapter of every title for free.

Magnetizing of Finemet-type alloys by magnetization rotation in weak fields

V A Kataev¹, Y N Starodubtsev^{1,2} and K O Bessonova¹

¹Boris Yeltzin Ural Federal University, Mira str.19, Yekaterinburg, 620002, Russia

²Gammamet Research and Production Enterprise, Tatishchev str. 92, Yekaterinburg, 620028, Russia

E-mail: vakataev@urfu.ru

Abstract. Magnetic properties of functional magnetic materials depend on the magnetization processes nature. Creation of amorphous and nanocrystalline alloys using the rapid quenching technology is the result of the latest advances in magnetic materials area. Although significantly different in structure, they show excellence properties. In this paper we will investigate the magnetization properties of the Finemet-type nanocrystalline alloys in the range of their initial permeability formation. We will show that due to low level of effective magnetic anisotropy, even in weak fields, magnetization can occur through reversible, hysteresis-free rotation of the domain's magnetization vector.

1. Introduction

Typically the magnetization process is studied together with the mechanisms change, i. e. as the magnetization field increases, first the domain walls are displaced, and later, their magnetization vector is rotated. Initially the domains magnetization is oriented along the easy magnetization axis (EMA). In weak magnetic fields, if the EMA and the field direction do not coincide, the magnetization occurs by the walls displacement of the domains with magnetization closest to the direction of the field. In strong fields, the resulting magnetization rotates in the direction of the field. However, such a scenario is caused considerably by a significant amount of magnetic anisotropy in traditional soft magnetic materials. In this case, the increase of magnetization due to the displacement of the domain walls requires less energy. The appearance of new materials with different structural condition recalled attention to the subject. Thus the magnetic anisotropy in amorphous and nanocrystalline alloys can be quite small due to the absence of magnetocrystalline anisotropy and/or its suppression by the mechanism of the random anisotropy model [1]. Herzer [1, 2] suggested that the magnetizing in the Finemet alloy samples appears to be a mixture of the magnetization rotation processes and of the domain walls displacement. The points of view differ a lot in some recent studies [3, 4] while describing the role of Finemet nanocrystalline alloys magnetizing by magnetization rotation. We have studied the magnetization process in a weak static magnetic field of samples of the $\text{Fe}_{67.5}\text{Co}_5\text{Cu}_1\text{Nb}_2\text{Mo}_{1.5}\text{Si}_{14}\text{B}_9$ alloy with uniaxial magnetic-field-induced anisotropy and without it.

2. Samples and methods

The ribbon samples of $\text{Fe}_{67.5}\text{Co}_5\text{Cu}_1\text{Nb}_2\text{Mo}_{1.5}\text{Si}_{14}\text{B}_9$ alloy were obtained by the ultrafast quenching method and wound into toroids. Then they were subjected to heat treatment for nanocrystallization,



combined or not with the application of a magnetic field. After nanocrystallization the natural magnetocrystalline anisotropy is averaged and the induced magnetic anisotropy plays the main role. The anisotropy axis of the type *L* sample was directed along the length of the ribbon; the anisotropy axis of the type *T* sample was directed perpendicular to the length of the ribbon; in the type *O* sample uniaxial anisotropy was absent. The type *L* and the type *T* samples were chosen because their magnetization processes in the field applied along the length of the ribbon are well defined. In the type *L* sample the applied field direction and the magnetization in the domains are parallel, and the magnetization process arises from displacing 180° domain walls. In the sample type *T* the magnetization in the domains and the field applied are perpendicular, and the magnetization process arises from magnetization rotation [5]. We shall study the peculiarities of magnetization process in the type *O* sample without uniaxial anisotropy. For comparison, we used the type *O* sample of $\text{Fe}_{72.5}\text{Cu}_1\text{Nb}_2\text{Mo}_{1.5}\text{Si}_{14}\text{B}_9$ alloy in which the induced anisotropy constant is noticeably inferior to the alloy containing cobalt.

The measurements were carried out using the MMKS magnetic measuring apparatus. The sample was demagnetized before measuring with a decaying alternating magnetic field of 1 Hz frequency. The magnetizing field was changed “in a step-like fashion” and the loops were obtained by a point-by-point procedure (ballistic method) [6]. This method allows accurate measurements in weak fields and at small inductions. It provides next relative errors in measuring of the magnetic quantities: magnetic field – 2 %, magnetic induction – 3 %, hysteresis losses – 5 %.

3. Results and discussion

In conventional soft magnetic materials, such as Fe-3%Si, heat treated appropriately, for samples cut along the easy magnetization axis, the magnetization curves are higher than for the samples cut at an angle or across the EMA. This reflects the easier magnetization process due to the displacement of 180° domain walls as compared to the displacement of the 90° domain walls or the magnetization rotation.

Figure 1a shows segments of magnetization curves of samples *L*, *T* and *O*. In magnetizing fields of ~ 3 A/m the standard placement of the curves is observed: the magnetization increases the most rapidly in the sample type *L*, magnetized by domain walls displacement, the sample type *O* occupies a middle position, the magnetization increases the most slowly in the sample type *T*, magnetized by coherent rotation of the domains magnetization vector.

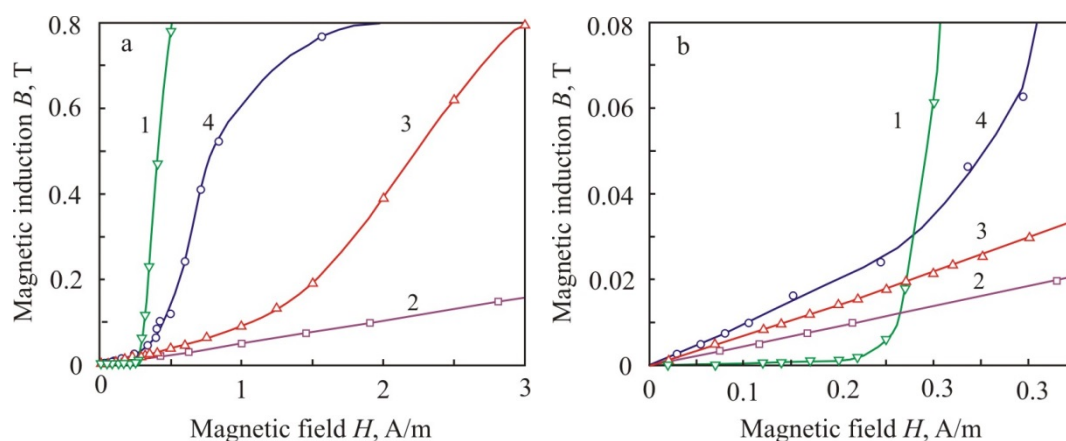


Figure 1. Magnetization curves of sample types *L* (1), *T* (2), *O* (3) of the $\text{Fe}_{67.5}\text{Co}_5\text{Cu}_1\text{Nb}_2\text{Mo}_{1.5}\text{Si}_{14}\text{B}_9$ alloy and sample type *O* of $\text{Fe}_{72.5}\text{Cu}_1\text{Nb}_2\text{Mo}_{1.5}\text{Si}_{14}\text{B}_9$ alloy (4) in the medium (a) and weak (b) magnetization fields region.

However, in the range of weak fields (figure 1, b), the relative position of the curves is different. The magnetization in the sample type *L* practically does not increase, revealing the effect of the fixing

domain walls mechanism. In the sample type *T*, the magnetization rotation provides an easy linear magnetization increase. As for the sample type *O*, the magnetization increases the most rapidly. It has no single axis anisotropy. Its domain structure is the most complex with randomly oriented magnetization of domains. As a result of the annealing of this sample, a local axis of induced anisotropy appears in each domain. Thus, there is a certain angle between the applied field and the direction of magnetization in any domain. Taking into account the easy of the rotation process in the sample type *T*, one can expect a significant role of the magnetization rotation during the magnetization of the sample type *O*. At the same time, the domain walls displacement cannot be excluded. If we take into account that the rotation process is reversible, i.e. it occurs without energy losses from hysteresis, in contrast to the displacement of domain walls, it means that by measuring the hysteresis losses, it will be possible to evaluate which of these processes plays a leading role in weak fields.

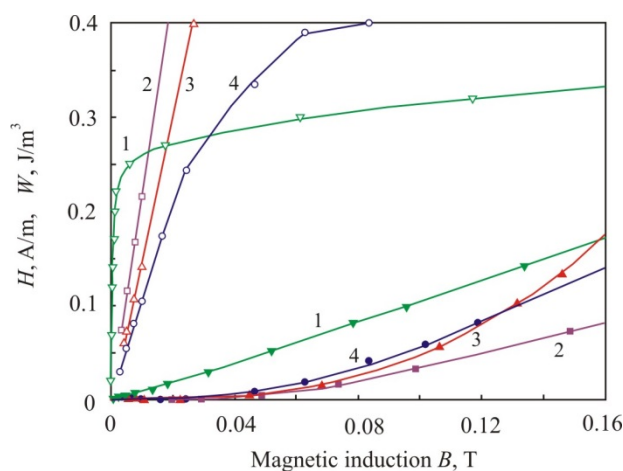


Figure 2. Dependence of hysteresis losses (filled points) in the sample types *L* (1), *T* (2), *O* (3) of the $\text{Fe}_{67.5}\text{Co}_5\text{Cu}_1\text{Nb}_2\text{Mo}_{1.5}\text{Si}_{14}\text{B}_9$ alloy, and the sample type *O* of the $\text{Fe}_{72.5}\text{Cu}_1\text{Nb}_2\text{Mo}_{1.5}\text{Si}_{14}\text{B}_9$ alloy (4) together with the magnetization curves of the same samples (empty points) in coordinates $H(B)$ in the weak magnetization fields region.

In figure 2, the hysteresis losses of sample types *L*, *T*, *O* for this region of the fields are shown as function of induction. The same figure presents for convenience, the magnetization curves of these samples in the coordinates $H(B)$. The sample type *L*, in which a slight induction increase is observed in the fields of about 0.25 A/m and its further rapid increase in the fields of more than 0.25 A/m, demonstrates the fastest hysteresis losses increase among all samples. Since the magnetization of this sample occurs due to the domain walls displacement process, this one is responsible for such hysteresis loss behaviour. Rapid induction increase is observed in the samples of types *T* and *O* in the weak fields region (figure 1b, curves 2, 3; figure 2, curves 2, 3 empty points), while the hysteresis losses in these samples (figure 2, curves 2, 3 filled points) turn out to be far smaller than in the sample type *L*. In the sample type *T*, the magnetization reversible process prevails due to the uniform rotation of magnetization of the domains to the field direction. As a result, despite the induction increase, the losses are close to zero up to 0.07 T. Then the losses increase very slightly, remaining much smaller than for the sample type *L*. The sample type *O* curves follow the same pattern as the sample type *T*. The losses remain close to zero up to 0.07 T and increase above 0.07 T (figure 2, curve 3). This would have been impossible if the processes of irreversible displacement of the domain walls, causing hysteresis losses, had played a significant role here. This result indicates that reversible rotation processes play a leading role in the sample type *O* in the weak fields region. Figures 1 and 2 also show the results for the type *O* sample of the nanocrystalline alloy without Co. It is known that the presence of Co atoms leads to the induced anisotropy constant increase. Therefore, we can expect to find a smaller induced anisotropy constant value in the alloy without Co. According to our assumption of the leading role of the rotation processes, it is expected that constant value decrease facilitates magnetization (curves 4 in figure 1b and figure 2). At the same time, the hysteresis losses in this sample, as in the sample type *O* with Co, remain insignificant (figure 2, curve 4, filled points),

indicating that the magnetizing of both samples occurs due to the reversible rotation of the magnetization.

The change in magnetization / permeability in the range of weak fields can be described using the Rayleigh law:

$$\mu = \mu_i + \eta H \quad (1)$$

where μ_i is the initial permeability, η is the Rayleigh constant, H is the magnetic field. The initial permeability is determined by reversible magnetization processes, the Rayleigh constant characterizes the linear contribution of the irreversible magnetization processes. The ratio between the initial permeability and the Rayleigh constant - the hysteresis factor [7] - reflects the ratio of the contributions of reversible and irreversible processes during magnetization.

Table 1. The Rayleigh law parameters.

Sample	μ_i	H	μ_i/η	H_{cr} , A/m
type <i>L</i> , $\text{Fe}_{67.5}\text{Co}_5\text{Cu}_1\text{Nb}_2\text{Mo}_{1.5}\text{Si}_{14}\text{B}_9$	1780	19730	0.09	0.22
type <i>T</i> , $\text{Fe}_{67.5}\text{Co}_5\text{Cu}_1\text{Nb}_2\text{Mo}_{1.5}\text{Si}_{14}\text{B}_9$	35820	2567	14.0	0.65
type <i>O</i> , $\text{Fe}_{67.5}\text{Co}_5\text{Cu}_1\text{Nb}_2\text{Mo}_{1.5}\text{Si}_{14}\text{B}_9$	53510	14340	3.7	0.67
type <i>O</i> , $\text{Fe}_{72.5}\text{Cu}_1\text{Nb}_2\text{Mo}_{1.5}\text{Si}_{14}\text{B}_9$	70830	48460	1.5	0.27

The table 1 shows the parameters of the Rayleigh law for all samples. It can be seen that for sample type *L* the contribution of reversible processes is very small, while for sample type *T*, on the contrary, it is significant. For the type *O* samples, the hysteresis factor value is significantly higher than for the sample type *L*, indicating that the proportion of reversible processes in the type *O* is considerably higher. This confirms the conclusion about the significant contribution of the reversible processes of uniform magnetization rotation to the nanocrystalline samples magnetization. The value of the H_{cr} field given in the table is the field above which the Rayleigh constant ceases to be permanent, indicating a change in the nature of the magnetization processes. Obviously, it is related to the growing contribution of the processes of domain wall displacement that increases one of the irreversible magnetization and diminishes the corresponding contribution of the reversible magnetization rotation. The table illustrates that this change occurs earlier for the sample type *O* without Co, than for the same sample type with Co. Perhaps this earlier H_{cr} value change explains the lower value of the hysteresis factor for this sample compared to the one with Co.

4. Conclusion

Thus, while increasing the magnetization field in the nanocrystalline alloys with low effective magnetic anisotropy and low induced anisotropy, we observe a different order of magnetization mechanisms change compared to one characterizing traditional soft magnetic materials. The magnetization process starts with a reversible magnetization rotation, supplemented later by an irreversible domain walls displacement. When the magnetization approaches the technical saturation, it increases again, apparently, due to the magnetization vector rotation, overcoming the local anisotropy forces significant in atomic scale.

Acknowledgments

This work was supported by the Ministry of Science and higher Education and of the Russian Federation in the framework of state tasks No. 3.6121.2017/8.9 and No. 4.9541.2017/8.9.

References

- [1] Herzer G 1997 *Handbook of Magnetic Materials* vol 10, ed K H J Buschow (Amsterdam: Elsevier Science B.V.) chapter 3 pp 415-62
- [2] Herzer G 2013 *Acta Materialia* **61** 718-34
- [3] Kovác J, Novák L. and Varga L K 2017 *Acta Physica Polonica A* **131** 732–34
- [4] Varga L K and Kovac J 2018 *AIP Advances* **8** 047205
- [5] Starodubtsev Yu N, Kataev V A, Bessonova K O and Tsepelev V S 2019 *J. Magn. Magn. Mater.* **479** 19–26
- [6] Fiorillo S 2004 *Measurement and Characterization of Magnetic Materials (Elsevier Series in Electromagnetism)* ed I Mayergoyz (Amsterdam: Elsevier Academic Press) p 340
- [7] Starodubtsev Yu N, Kataev V A and Tsepelev V S 2018 *J. Magn. Magn. Mater.* **460** 146–52